International Journal of Nanomedicine

Dovepress
open access to scientific and medical research

Open Access Full Text Article

ORIGINAL RESEARCH

Berberine-Loaded Thiolated Pluronic F127 Polymeric Micelles for Improving Skin Permeation and Retention

This article was published in the following Dove Press journal:
International Journal of Nanomedicine

Jiangxiu Niu[1,*]
Ming Yuan[1,*]
Chenchen Chen[1]
Liye Wang[1]
Zigui Tang[2]
Yanli Fan[1]
Xianghui Liu[1]
Yu Jiao Ma[1]
Yu Gan[1]

[1]College of Food and Drug, Luoyang Normal University, Luoyang 471934, People's Republic of China; [2]Department of Pharmacy, Henan Medical College, Zhengzhou 451191, People's Republic of China

*These authors contributed equally to this work

Background: Challenges associated with local antibacterial and anti-inflammatory drugs include low penetration and retention of drugs at the expected action site. Additionally, improving these challenges allows for the prevention of side effects that are caused by drug absorption into the systemic circulation and helps to safely treat local skin diseases.

Methods: In the current study, we successfully prepared a thiolated pluronic F127 polymer micelles (BTFM), which binds to keratin through a disulphide bond, to produce skin retention. In addition, the small particle size of polymer micelles promotes the penetration of carriers into the skin. The current study was divided into two experiments: an in vitro experiment; an in vivo experiment that involved the penetration of the micelle-loaded drugs into the skin of rats, the skin irritation test and the anti-inflammatory activity of the drug-loaded micelles on dimethyl benzene-induced ear edema in mice.

Results: Results from our in vitro transdermal experiment revealed that the amount of drug absorbed through the skin was decreased after the drug was loaded in the BTFM. Further, results from the vivo study, which used fluorescence microscopy to identify the location of the BTFM after penetration, revealed that there was strong fluorescence in the epidermis layer, but there was no strong fluorescence in the deep skin layer. In addition, the BTFM had a very good safety profile with no potentially hazardous skin irritation and transdermal administration of BTFM could significantly suppress ear edema induced by dimethyl benzene. Therefore, these findings indicated that BTFM reduced the amount of drug that entered the systemic circulation. Our results also demonstrated that the BTFM had a certain affinity for keratin.

Conclusion: Our experimental results suggest that the BTFM may be an effective drug carrier for local skin therapy with good safety profile.

Keywords: F127 polymeric micelles, berberine, cysteine, skin permeation and retention

Introduction

Berberine hydrochloride (BH), or berberine, is an isoquinoline alkaloid that has a strong antibacterial ability, broad antibacterial spectrum, and wide application prospect in the treatment of bacterial and fungal infections and other skin diseases.[1,2] However, berberine has low solubility, poor membrane permeability, and low bioavailability. Therefore, it is necessary to develop advanced preparations of berberine to improve its therapeutic efficiency. Recently, selenium-coated nanostructured lipid carriers were developed for enhancing the oral bioavailability and the curative effect of berberine, and the developed nanoparticles resulted in

Correspondence: Liye Wang; Zigui Tang
Email liye2009314@163.com; 453869820@qq.com

enhanced oral bioavailability of berberine compared with the berberine solution.[3] Nanostructured lipid carriers were also developed as a delivery system for enhanced anti-inflammatory activity of berberine against ulcerative colitis.[4] In addition, injectable in situ forming gels for sustained release of berberine against sodium nitroprusside-induced apoptosis of chondrocytes were developed to improve the antiapoptotic efficiency of berberine.[5] Because of low penetration into skin of berberine, current marketed powders and ointments do not accumulate in high concentrations in the skin tissue and stay for a long time. Recently, to increase the skin bioavailability of berberine, Giulia Vanti and his research group prepared berberine-loaded escinosomes, and they proved that hydrogels formulated with berberine-loaded escinosomes had the highest berberine skin absorption both in terms of absorbed dose and of dose retained inside the skin.[6,7] Therefore, a novel formulation that improves the skin permeability and retention of BH would greatly increase the antibacterial effects of the drug and the compliance of patients.

Transdermal drug delivery is used to deliver drugs through human skin absorption. For the local drug delivery systems (DDS) of skin, improving skin retention could improve the treatment effect and reduce the amount of drug entering the blood circulation, thereby avoiding the toxic and side effects. Additionally, studies have reported that preparing appropriate dosage forms of drugs to treat skin diseases is an effective way to increase skin retention and reduce the amount of drugs that enter the blood circulation.[8,9] Local antifungal therapy requires high drug concentrations in skin tissue and reduced systemic absorption of the drugs in order to reduce adverse reactions. The development of new drug carriers is conducive to the penetration of drugs into the skin and may help control and sustain the release of drugs. By providing controlled and sustained release of drug reserves at the infected site, drug loading systems act as a reservoir that achieves drug enrichment at the drug delivery site and reduces drug concentration in the circulatory system. For example, studies have verified that the colloidal drug delivery system, including microemulsions, nanoemulsions, and micelles; vesicle drug delivery system, including liposomes, alcohol liposomes, liposome-like structures, and transporters; and nanoparticle drug delivery system, including solid lipid nanoparticles and nanostructured liposomes, promote skin penetration and retention of drugs.[10–13]

Polymer micelles are colloidal solutions with core-shell structures that are formed by the self-assembly of amphiphilic copolymers above the critical micelle concentration. They are often used as carriers of water-insoluble drugs and have good biocompatibility.[14] Additionally, aqueous polymer micellar nanoformulations encapsulate the drug in the hydrophobic inner core of the micelles and away from the aqueous solution in order to enhance the stability of the drug.[15] When small-size micelle particles come into contact with the lipophilic stratum corneum, they may promote drug adsorption and penetration through the stratum corneum through hydration and promote drug penetration into the skin.[16] In addition, polymer micelles can be modified by chemical structure to improve their skin permeability.[17] Acetylation or carboxylation modification on the surface of micelles can enhance skin penetration and allows them to spread more easily throughout the intercellular pathway. Conversely, amino-terminated polymers retain drugs in cells and skin but reduce drug penetration into the skin.[18] Furthermore, combining polymers with octadecenoic acid can enhance skin absorption and retention. Therefore, polymer micelles reduce the toxic and side effects of drugs, maintain the drug concentration within the therapeutic concentration range for a long time, and have certain skin penetration and retention effects.[19] The development of polymer micelles is considered to be one of the effective way to selectively target drugs to the local skin.[20]

Thiolated polymers have been widely used to improve the oral bioavailability of drugs,[21–23] prolong delivery of drugs to mucosal membranes,[24] prolong nanoparticles retention at the tumor site,[25] and restore hair.[26] Skin keratin is the main structural protein of epidermal cells, and the structure of skin keratin is rich in cysteine. Polymers that contain thiol groups can improve their adhesion to skin tissue by forming disulphide bonds with cysteine in keratin. As a non-ionic block copolymer, poloxamer F127 has good biocompatibility, is non-toxic, and is easy to obtain. In this study, we synthesised an L-cysteine modified poloxamer F127, and the copolymer was used as the carrier material to prepare thiolated amphiphilic drug-loaded nanomicelles. Through the binding with keratin or hydration with skin, the micelles function to permeate the membrane and biologically adhere to the skin, which promotes drug penetration into the skin and increases the amount of retention in the skin (Figure 1). This ultimately reduces the amount of drugs that enter the systemic circulation and enhances the therapeutic effects of superficial

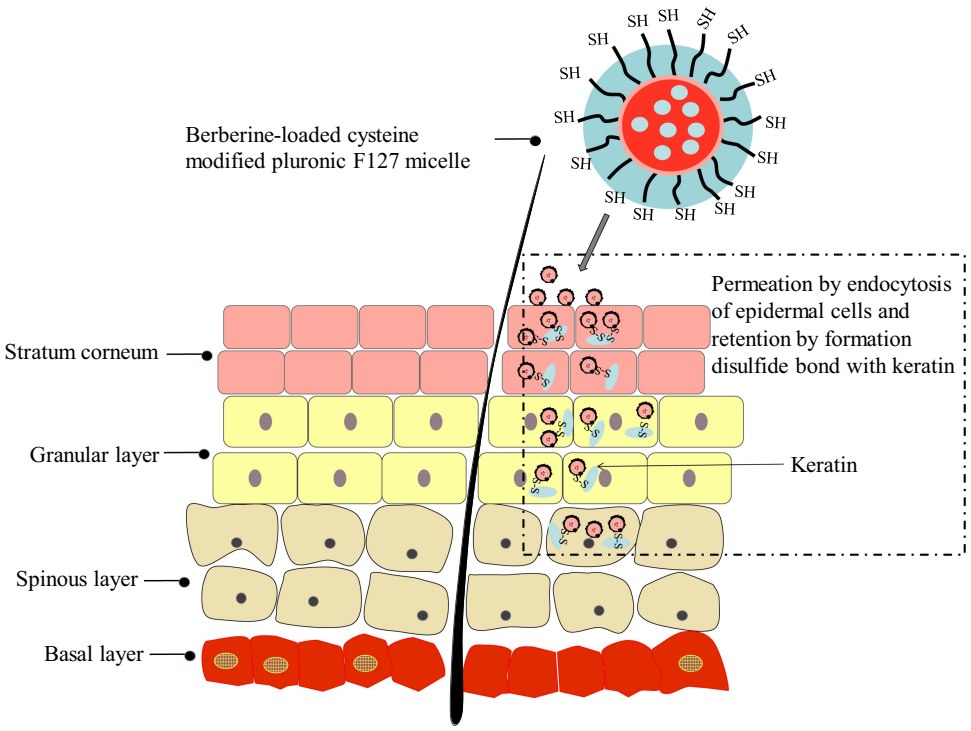

Figure 1 Representation of the strategy of developing berberine-loaded cysteine-modified pluronic F127 micelle for improving skin permeation and retention.

bacterial or fungal infections. Therefore, this study focused on the preparation and characterisation of berberine hydrochloride-supported thiolated F127 micelles. Additionally, we studied the skin penetration and retention effects of the preparations through in vitro transdermal experiments and fluorescence microscopy.

Materials and Methods

Materials

Pluronic F127 was purchased from BASF (Shanghai, China). Coumarin-6 and L-cysteine were purchased from Hefei Bomei Biotechnology Co., Ltd (Hefei, China). 1-(3-dimethylaminopropyl)-3-ethylcarbodiimide hydrochloride (EDC. HCL) and N-hydroxysuccinimide (NHS) were purchased from Nanjing Dulai Biotechnology Co., Ltd (Nanjing, China). 5,5′-Dithiobis-(2-nitrobenzoic acid) (DTNB) was purchased from Fuyang Manlin Biotechnology Co., Ltd (Fuyang, China). BH was purchased from Shanghai Siyu Chemical Technology Co., Ltd (Shanghai, China). All other reagents were analytical grade preparation. Distilled or deionised water was used in all experiments.

Animals

We obtained Sprague Dawley (SD) rats (approximately 180–220 g in body weight) and and Male ICR mice (approximately 18–22 g in body weight) from the Henan Experimental Animal Center, Zhengzhou, China. All of the animals were housed in temperature-controlled (23–25°C) rooms under a 12 h light cycle and had free access to food and tap water before the experiment. Animal experiments were carried out in accordance with the guidelines approved by Luoyang Normal University, and the study was approved by the Institutional Animal Ethics Committee.

Synthesis of Cysteine Conjugated Pluronic F127

In order to obtain carboxylated active groups for conjugated cysteine, a carboxylic acid end-standing pluronic F127 was initially obtained. Briefly, 6 mL of 3.8% $KMnO_4$ solution was added to a solution of pluronic F127 (2.0 g, 0.16 mmol) in a mixed solvent of deionised water (30 mL) and diluted H_2SO_4 (0.2 mL). The reaction was carried out for 30 min at 25°C under stirring conditions. Then, the terminal carboxylated pluronic F127 was dialysed (MWCO 3500Da) against deionised water for 3 days for purification, and the white powder of the carboxylated pluronic F127 was obtained by freeze drying.

Cysteine conjugated pluronic F127 was synthesised by incorporating cysteine into the terminal carboxyl groups in the carboxylated pluronic F127. Briefly, the carboxylated

pluronic F127 (1 g, 0.8 mmol) was dissolved in 30 mL of phosphate buffer solution (PBS; pH 6) that contained EDC (98 mg, 0.45 mmol) and NHS (52 mg, 0.45 mmol) as catalytic agents. Then, cysteine (71 mg, 0.45 mmol) was added to the mixture and stirred at room temperature for 3 h. The resulting mixture was filtered and dialysed against deionised water for 3 days in the dark, and the final product was obtained by lyophilisation.[27] The chemical structure of the product was identified by ^{1}H NMR using a 400 MHz apparatus (AVANCE500, Bruker, Germany) at 25°C, the product was dissolved in D_2O to achieve a concentration of 10 mg/mL. ^{13}C NMR spectra were measured on a Bruker AVANCE500 NMR spectrometer at 400 MHz in DMSO-d_6.

Determination of Thiol Group Content

The amount of free thiol groups that was attached to the thiolated pluronic F127 was quantified spectrophotometrically via Ellman's reagent (5,5 dithiobis 2-nitrobenzoic acid, DTNB) according to the literature.[24,27] First, 7.3 mg of the cysteine conjugated pluronic F127 was completely dissolved in 0.5 mL of 0.5 mol/L PBS (pH=8.0). Subsequently, 0.5 mL of Ellman's reagent (DTNB dissolved in 0.5 mol/L PBS) was added to the solution, and the reaction was conducted at room temperature for 2 h in the dark. Next, the solution was centrifuged for 15 min at 12,000 r/min, and the absorbance of the supernatant was determined at 412 nm using a microplate reader (PerkinElmer VICTOR Nivo, Finland).

The amount of modified thiol groups was calculated according to a standard curve, which was established according to the L-cysteine concentration (C) and the corresponding absorption (A) with a correlation coefficient of 0.9953.

Preparation of Berberine-Loaded Micelles

Berberine-loaded micelles were prepared via the thin film hydration method. Briefly, 8 mg of berberine and 100 mg of thiolated pluronic F127 were co-dissolved in 20 mL absolute alcohol in a round-bottom flask and sonicated for 30 min. The absolute alcohol was evaporated at 45°C by rotary evaporation, and the thin film was obtained and placed in a vacuum dryer to further remove the residual organic solvents by vacuum drying overnight at room temperature. Next, the dried thin film was hydrated with 30 mL deionised water at 37°C for 1 h to obtain berberine-loaded thiolated pluronic F127 polymeric micelles (BTFM) solution. Then, the unincorporated drug was removed by filtrating the solution through a 0.22 μm microporous membrane (Millex LCR hydrophilic, Millipore Co.). The berberine-loaded pluronic F127 micelles (BFM) were prepared using same method that was described above; however, thiolated Pluronic F127 was replaced with pluronic F127.

Characterisation of Berberine-Loaded Micelles

Drug Loading and Encapsulation Efficiency

The drug concentrations of berberine in the polymeric micelles were extracted with absolute ethanol and determined using an ultraviolet-visible spectrophotometer (TU-1810PC, Purkinje, Beijing, China) at 350 nm. The content determination method was calibrated using standard solutions at different concentrations that ranged from 2 to 10 μg/mL of berberine that was dissolved in absolute ethanol (R^2= 0.9981). The drug loading content (DL) refers to the percentage of the weight of the drug-loaded in the micelles relative to the total weight of the feeding polymers and drug, and the entrapment efficiency (EE) refers to the percentage of the drug encapsulated in the micelles relative to the weight of feeding drug. Therefore, the DL% and EE% of berberine in micelle preparations were calculated according to the following equations:[28]

$$DL\% = \frac{\text{Weight of the drug loaded in micelles}}{\text{Weight of the feeding polymers and drug}} \times 100\%$$

$$EE\% = \frac{\text{Weight of the drug encapsulated in micelles}}{\text{Weight of the feeding drug}} \times 100\%$$

Particle Size Distribution and Zeta Potential Measurement

The drug-loaded micelles were filtered through a 0.22 μm disposable membrane before measurement, and the samples were diluted to a polymer concentration of 8 mg/mL in deionised water for determination. The hydrodynamic diameters, particle size distribution and zeta potential of drug-loaded micelles were obtained using the Zetasizer-3000 dynamic light scattering (DLS) instrument (Malvern Instruments, UK) at 25±0.1°C after equilibration for 2 min. Additionally, the He-Ne laser was set to 633 nm, and the angle was fixed at 90°.[29] The measurements

were repeated in three independent samples to obtain the average value.

Morphology Examination

TEM was employed to observe the morphological features of the berberine-loaded micelles. TEM images of the micelles were recorded using a JEM-100CX electron microscope (JEOL, Tokyo, Japan) instrument at 120 kV. Micelles were diluted to a concentration of about 1 mg/mL with deionised water before investigation. A drop of diluted micelles was deposited on a carbon-coated copper grid, and excess liquid was removed from the sides of the copper disc using fine filter paper. Next, the sample was negatively stained with a drop of 2% (w/v) phosphotungstic acid. The grid was thoroughly washed with deionised water to remove excess stain and dried at room temperature for about 10 min before viewing under the TEM.

The surface morphology of the berberine-loaded micelles was also evaluated under a scanning electron microscope (SEM) (Sigma 500, ZEISS, Germany). For this purpose, the SEM samples were prepared by coating 0.1 mg/mL micelle suspensions on silicon substrate and coated with gold of 10 nm thickness using a sputter coater under vacuum for allowing visualization. Then, images of the samples were taken by applying an acceleration voltage of 5.0 kV and 5.0 mm working distance to identify the surface of the formulation.

Differential Scanning Calorimetry (DSC)

The thermal analysis of berberine, cysteine conjugated pluronic F127, physical mixtures of drugs and carriers, and lyophilised drug-loaded micelles was determined using the Q2000 modulated differential scanning calorimeter (TA instruments, America). Approximately 5 mg of each sample was placed in the aluminium pans, and the empty aluminium pans were recorded as the reference standard. The samples were scanned at a temperature that ranged from 30 to 300 °C at a heating rate of 10°C per min. The analysis was carried out under a dynamic nitrogen atmosphere.[30]

X-Ray Diffraction (XRD)

The XRD patterns of berberine, cysteine conjugated pluronic F127, and lyophilised drug-loaded micelles were determined using an X-ray powder diffractometer (D8 ADVANCE, Bruker, Germany). Copper kalpha radiation was used to substantiate probable drug carrier interactions. Additionally, the scanning rate was 5°C/min, and the working voltage and current were 40 kV and 40 mA, respectively. Diffraction patterns were collected at 5–70° with 2θ.

Fourier Transform Infrared Spectroscopy (FTIR)

A Nicolet 6700 Fourier transform infrared spectrophotometer (Thermo Fisher Scientific, USA) was also used to characterize the status of berberine in polymeric micelles. The infrared spectrograms were recorded using the KBr method in the range of 4000–400 cm^{-1}. Fourier transform infrared (FTIR) spectra of berberine, physical mixture of berberine and cysteine conjugated pluronic F127, berberine-loaded micelles (BTFM) and corresponding empty blank micelles were recorded at room temperature.

In vitro Release of Berberine-Loaded Micelles

We investigated the concentration of berberine that was released from the micelles in vitro using a dynamic state membrane dialysis method that employed a dialysis bag with an average flat width of 28 mm. PBS (pH 7.4 and pH 5.5) was used as the release medium. Briefly, 1 mL of the berberine-loaded micelle suspension was transferred into a dialysis bag with MWCO 3.5 kDa, and the end-sealed dialysis bag was immersed in 50 mL of release medium that was maintained at 37±0.1°C and shaken at 100 rpm. Next, 1 mL of the sample was removed from the release medium for content determination at the following time points: 0.25, 0.5, 075, 1, 2, 4, 6, 8, 10, 12, and 24 h, and an equal volume and temperature of fresh medium was appended into the system. The concentration of berberine in the withdrawn samples was assayed using the ultraviolet-visible spectrophotometer method described above. Various kinetic equations were used to fit the drug release behaviour in vitro to study the drug release mechanism from micelles.[31] Further, the cumulative release percentage of berberine at each time point was calculated using the following formula based on the total drug content:[32,33]

$$\text{Cumulative release}(\%) = \frac{C_n \times 50\text{mL} + \sum_{n=0}^{n-1} C_{n-1} \times 1\text{mL}}{\text{initial amount of berberine in the dialysis bag}}$$

where C_n and C_{n-1} represent the concentration of berberine in the release medium at the nth and n−1th time points, respectively.

In vitro Skin Permeation and Retention Studies

Preparation of Rats Skin

The rat abdomen skin was used for the in vitro skin permeation/retention studies.[34,35] Female SD rats weighting 200±20 g were purchased from Henan Experimental Animal Center. Animal experiments were conducted in accordance with the guidelines for the use and care of experimental animals approved by the Animal Ethics Committee of Luoyang Normal University. The rats were anaesthetised with ether, and the abdominal hair was carefully removed with a razor. The rats were executed by ether anaesthesia after 24 h of feeding, then the whole abdominal skin was removed immediately, and the subcutaneous tissue and excess fat were carefully removed. The side of stratum corneum was gently rinsed with saline, and the excised skin was wrapped in aluminium foil and stored in an ultra-low temperature refrigerator at −80°C until use. The skin was removed from the refrigerator and thawed at room temperature for at least 8 h, and the appropriate size of unharmed skin was selected under the anatomical microscope for use.[36]

Skin Permeation and Retention Studies

The skin permeation and retention studies were carried out under non-enclosed conditions by fixation of skin to a drug transdermal diffusion instrument (RYJ-6B, Shanghai, China) with an exposed area of 2.8 cm^2 and a receptor capacity of approximately 6.5 mL. Briefly, round skin specimens were carefully immobilised on the receptor chamber of the transdermal diffuser with the stratum corneum facing the donor chamber of the diffusion cell. The receptor chamber was filled with the receiving medium (PBS, pH 7.4), heated to 37°C in a water bath to correspond to the normal skin temperature of human body, and continuously stirred at a speed of 300 rpm. Next, 500 μL of the berberine-loaded thiolated pluronic F127 polymeric micelles (BTFM), berberine-loaded pluronic F127 micelles (BFM), or berberine solution were added to the skin. Subsequently, 1.0 mL of the samples was withdrawn at the following time intervals of 0.5, 1, 2, 3, 4, 5, 6, 7, 8, 10, and 24 h and immediately replaced with an equal volume of fresh receptor fluid to maintain a constant volume. Then, the samples were analysed using a high-performance liquid chromatography (HPLC) system (U-3000, Thermo, USA) with a UV detector and a Wondasil C18 column (5 mm, 200×4.6 mm). The mobile phase consisted of acetonitrile, water, and phosphoric acid at a ratio of 21:79:0.4 (v/v/v). The UV visible detector and operating temperature were set to 240 nm and 30°C, respectively. The flow rate was 1.0 mL/min and injection volume was 20 μL. Each preparation was analysed three times, and the cumulative amounts of berberine that permeated through the rat skin were plotted as a function of time.

To investigate drug retention in skin, the skins were removed from the diffusion instrument at 24 h after the permeation experiments and rinsed with deionised water to remove the excess preparation. Then, nine full-thickness skins were, respectively, cut into pieces with scissor and homogenised in 5 mL of methanol. The tissue homogenate was immediately separated by centrifugation at 12,000 rpm for 10 min, and the total amount of berberine extracted from skin at the end of the permeation study (24 h) was obtained from the concentration of berberine in supernatant methanol. The content of berberine in the extracted skin was determined using HPLC as described above.

In vivo Percutaneous Permeation of Fluorescent Probe-Labelled Micelles in Rats

In order to better study the permeability of functional micelles to living skin, coumarin-6 was used as fluorescence probe. Fluorescence probe-loaded thiolated pluronic F127 polymeric micelles (FTFM) and pluronic F127 micelles (FFM) were prepared by thin film evaporation as described above, and the transdermal penetration in the skin was studied in vivo. One day before the experiment, the rats were intraperitoneally anaesthetised with 1% phenobarbital sodium, and their back hair was removed. Next, 200 μL of the fluorescent probe-loaded micelle solution was applied onto a 1.5 cm^2 non-woven absorbent cotton sheet on three depilated skin sites of rats. After 0.5, 1.0, and 2.0 h of application, the cotton sheet and the residual fluorescent probe formulation on the skin sample were removed by rinsing with de-ionized water, the rats were killed immediately by dislocation, and the skin at the site of administration was subsequently removed. Next, each skin sample was frozen at −80°C. The frozen samples were longitudinal-sections sliced at 8 μm thickness by a freezing slicer (Leica CM1950, Germany). Finally, the samples were imaged using an inverted fluorescence microscope (Leica DMI 3000B, Germany), and the green

fluorescence from coumarin-6 was used to establish the skin distribution of the micelles.

Mechanisms Underlying the Interaction Between Thiolated Pluronic F127 Micelles and Keratins

The interaction between micelles and keratin was also studied using a TEM, DLS instrument, and contact angle analyser.

The TEM observation was performed as described above. Next, keratin was extracted from human hair using the reduction method to retain more free thiol groups,[37] and the keratin was dissolved in deionised water at a concentration of 0.5 mg/mL. The insoluble impurities were removed by centrifugation at 3000 rpm for 20 min and magnetically stirred for 1 h at room temperature. The keratin solution was mixed with BTFM at equal volumes and incubated in a shaker at 100 rpm at 37°C for 1 h, and the mixture was detected by TEM.

Particle size and zeta potential measurements were also used to evaluate the interaction between keratin and BTFM. The keratin was precisely weighed and dissolved in a PBS buffer solution (pH 7.4) to form a 0.5 mg/mL solution. The impurities of keratin solution were removed by centrifugation at 3000 rpm. Next, the keratin solution was mixed with BTFM solution by volume ratio of 1:10, 1:5, and 1:1, respectively. Then, the mixed solution was incubated in a shaker at 100 rpm at 37°C for 1 h, and the Zetasizer-3000 DLS instrument was used to measure the particle size and zeta potential different proportions of the mixed solution.

The surface wettability of keratin and BTFM was determined by contact angle (θ) measurement (DSA-200, Beito Science, China). Briefly, a 100 mg/mL keratin solution was evenly laid on a smooth glass plate with an area of 1 cm^2. The glass plate was placed in an oven at 37°C until the liquid was evaporated and dried. Then, a 15 μL drop of micelles was placed onto the surface of keratin coated glass slides, and the contact angle was measured and recorded by the DSA-200 instrument. We averaged three measurements from different areas of the surface to obtain the contact angle.

Acute Dermal Irritation Test

The dermal irritation/corrosion properties of the developed formulation were assessed in mice according to the methods previously described in the literature with some modifications.[38,39] Mice were anesthetized by intraperitoneal injection of 2% chloral hydrate (0.15 mL/10 g) and their two sides of the spinal (approximately 3 cm^2) were shaved 24 h before the test without causing tissue damage. Subsequently, filter papers (2 cm^2) were impregnated with 0.2 mL of formulation and then positioned on the dorsum of the mice, and fixed with hypersensitive tape. After 4 h of administration, the residual samples were removed with warm water. At 1, 4, 24 and 72 h after removing the residual samples, the skin irritation properties such as erythema and edema were observed. Physiological saline was used as negative control, and each group consisted of six animals.

Dimethyl Benzene Induced Mice Ear Edema

The anti-inflammatory effect of the developed formulation was assessed in acute inflammation method described with slight modifications.[40,41] Mice were transdermal administered with the formulation after 60 min, dimethyl benzene (40 μL per mouse) was applied to both surfaces of the right ear, and the left ear was used as the control. After 30 min of dimethyl benzene application, the mice were sacrificed by cervical dislocation. The right and left ears were cut off at the same position with an 8 mm stainless steel mouse ear puncher and weighed. The weight of ear edema and the rate of inhibition were evaluated by the following formula:

Edema weight = weight of the right ear – weight of the left ear

Inhibition rate (%) = [(edema weight of control group – edema weight of treated group)÷ edema weight of control] × 100%

Data Analysis

All results were measured at least three times and data were expressed as the mean±standard deviation. A Student's *t*-test was used to compare differences between the two groups, and $P < 0.05$ was considered statistically significant.

Results and Discussion

Synthesis and Characterisation of Cysteine Conjugated Pluronic F127

The cysteine conjugated pluronic F127 was synthesised by conjugating cysteine to carboxylated pluronic F127 using EDC and NHS as catalytic agents (Figure 2A). The

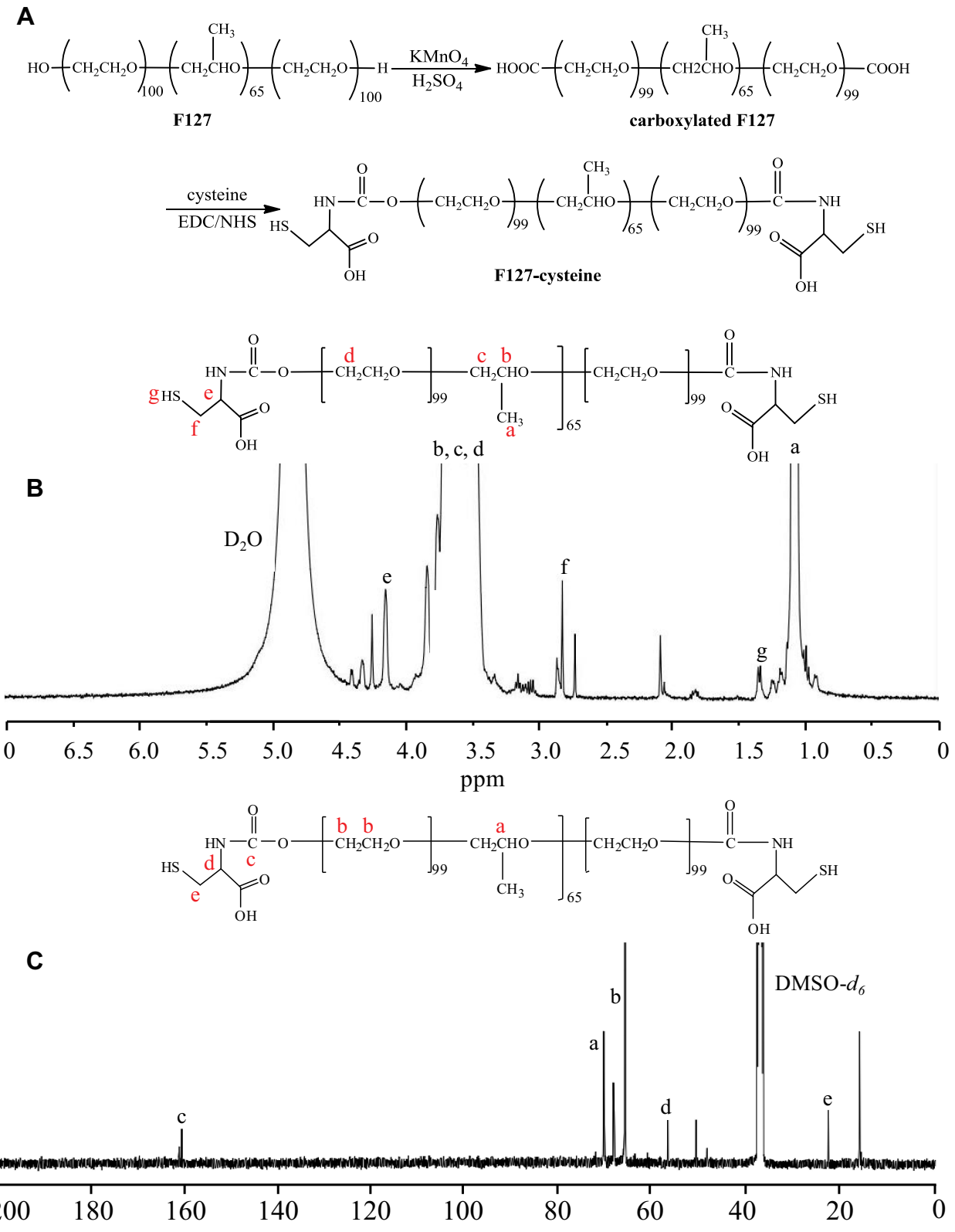

Figure 2 (**A**) Synthetic scheme. (**B**) ^{1}H NMR spectrum of the F127-cysteine. (**C**) ^{13}C NMR spectrum of the F127-cysteine.

chemical structure of cysteine conjugated pluronic F127 was identified by ^{1}H NMR (400 MHz, D_2O) and is displayed in Figure 2B. The peaks at δ (ppm) were 1.02 (d, 3H, -CH_3 of PPO), 3.30–3.65 (m, 3H, 4H, -CH_2CHO of PPO and -CH_2CH_2O- of PEO), 2.68–2.90 (m, -CH_2- of cysteine), 4.16 (s, -CH- of cysteine), and 1.32 (t, -SH of cysteine). ^{1}H NMR confirmed that the cysteine successfully conjugated to the pluronic F127.

The structure of cysteine conjugated pluronic F127 was also supported by the ^{13}C NMR (400 MHz, DMSO-d_6) characterizations. It can be concluded from the ^{13}C NMR spectra (Figure 2C) that the two signals detected at 22.46 ppm and 56.72 ppm were associated with methylene and methyne in cysteine groups, respectively, which were introduced into the carboxylated pluronic F127 by the amide reaction; the peak at 161.91 ppm was attributed to the carbonyl carbons of amide group; the other signals in the spectrum were ascribed to the carbon atoms in the repeating unit of F127. The ^{13}C NMR spectrum further confirmed that the cysteine successfully conjugated to the pluronic F127.

The amount of free thiol groups attached to the pluronic F127 was determined using the Ellman method, and the results showed that 1 g of thiolated pluronic F127 contained approximately 1.6×10^{-6} mol of thiol groups. The high modification degree of cysteine was an essential factor for the enhanced topical skin retention of the thiolated pluronic F127 polymers.

Characterisation of Berberine-Loaded Micelles

DL and Encapsulation Efficiency

In the present study, berberine was loaded in the core of thiolated pluronic F127 micelles to improve dermal targeting. They are also the key to improving the drug treatment index, reducing side effects of drugs, and reducing drug dosage. In order to increase DL and EE, drug-loaded micelles were prepared using thin film evaporation method, which facilitates the physical incorporation of hydrophobic drugs within the core of polymer micelles through the hydrophobic interactions between drugs and polymers.

In addition, the DL and EE of micelles can also be affected by the weight of the feeding drugs. Therefore, the effects of different weights of feeding drugs were investigated while the other conditions were fixed in the preparation of micelles (Figure 3). Overall, the results showed that

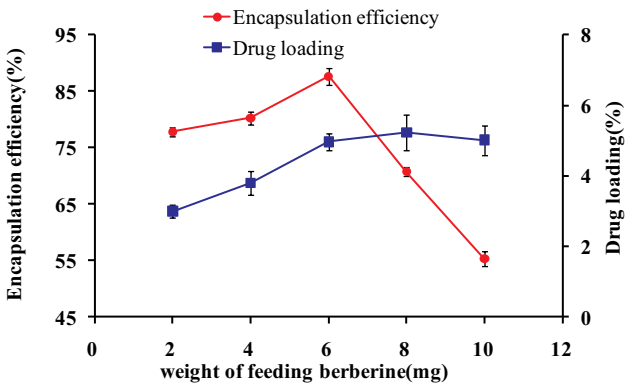

Figure 3 Effects of different proportions of drugs and carriers on encapsulation efficiency and drug loading (n=3).

the DL increased from 3.0% to 5.0% when the weight of the feeding drugs increased from 2 mg to 10 mg; however, the EE of the micelles was significantly decreased when the amount of berberine used for the preparation increased ($p<0.05$). Additionally, the EE reached the highest value (87.65%±1.52) when the weight of the feeding drugs was 6 mg. Therefore, the micelle formulations exhibited increased DL but decreased EE with increased drug feeding. This may be due to the saturation of berberine in the hydrophobic micelle core during the process of micelle formation, which resulted in excessive drug deposition on the surface of the micelles.[14,42] Therefore, the micelle formulation with 6 mg of feeding was used as the formulation in further studies. Additionally, preparations of berberine loaded thiolated pluronic F127 micelles indicated the prospect for a broad application with good DL properties.

Particle Size and Zeta Potential of Micelles

The mean particle diameter, size distribution, and zeta potential of micelles were measured using DLS. The size distribution of the BTFM exhibited a unimodal distribution (Figure 4A), which indicated that the expected monodisperse nano-scale micelles were formed. The particle size and zeta potential of micelles are summarised in Table 1. As shown in Table 1, the particle size (diameter) of the BTFM was approximately 9.7 nm, and the particle size was slightly increased as compared with that of the blank micelles. This was probably due to the fact that berberine was physically embedded in the hydrophobic inner core of the micelles. The polydispersity index (PDI) reflects the degree of uniformity of particle size

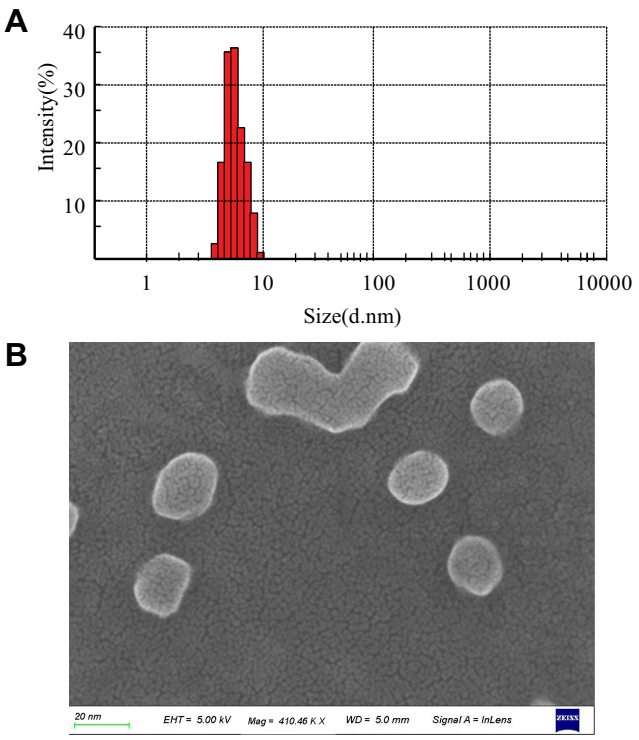

Figure 4 (**A**) Particle size and distribution of BTFM measured by DLS. (**B**) SEM images of BTFM.

distribution, and the smaller the PDI value, the narrower the particle size distribution and the more uniform the particle size.[30] PDI values in all formulations were smaller than 0.3, indicating that the size distribution of the measured micelles were narrow.[43]

The zeta potential is generally used to evaluate or predict the physical stability of the particle dispersion system, and a high zeta potential (>|20| mV) provides an electrostatic repulsion force between particles in order to avoid particle aggregation and growth.[44] The zeta potentials of the blank micelles, BFM, and BTFM were −0.58, −0.51, −27.01 mV, respectively. Compared with blank micelles, the BFM had almost no change in potential value; therefore, the encapsulation of berberine in the micelles did not affect the zeta potentials of the micelles. Conversely, the zeta potential of the BTFM was significantly lower than that of the BFM and blank micelles ($P<0.05$). This difference may be due to the presence of the carboxyl groups from the cysteine and carboxylated Pluronic F127 on the surface of the BTFM.

Table 1 Particle Size and Zeta Potential of Blank Micelles, BFM and BTFM

Types of Micelles	Particle Size (nm)	Zeta Potential (mV)	PDI
Blank micelles	8.92±0.42	−0.58±0.13	0.097±0.018
BFM	9.50±0.28	−0.51±0.18	0.181±0.034
BTFM	9.70±0.31	−27.01±0.20	0.195±0.029

Morphological Analysis

SEM images of BTFM (Figure 4B) showed spherical and uniform distribution of micelles with particle size about 10 nm. Figure 5A shows the TEM image of BTFM. As observed, the drug-loaded micelles were also polydispersed and spherical in shape grain like morphology with the particle size of between 5 and 20 nm. The obtained morphological results were in agreement with the earlier report, mostly drug-loaded pluronic polymer micelles are in spherical shapes.[45,46] The estimated particle size from SEM and TEM images was in good agreement with that measured by the DLS technique.

DSC Investigations

The existing status of the drug in the nanocarrier is of great significance to DDS. DSC is a tool that is used to rapidly acquire the existing forms of drugs in preparations and is based on changes in the thermal profile.[47] Thus, the berberine powder, cysteine conjugated pluronic F127, lyophilised BTFM, and its corresponding physical mixtures were analysed by DSC to evaluate the phase transition of berberine during the formation of the micelles. As shown in Figure 6, the DSC curve of berberine showed three sharp melting endothermic peaks at 133°C, 190°C and 287°C, which indicates that there are three crystal forms in the berberine raw materials.[48] The DSC curves of the physical mixtures showed the characteristic peaks of drug; however, the intensity was low (due to dilution), indicating that the drug retained its crystallinity in the physical mixture. In addition, the DSC curve of the physical mixtures showed a sharp melting

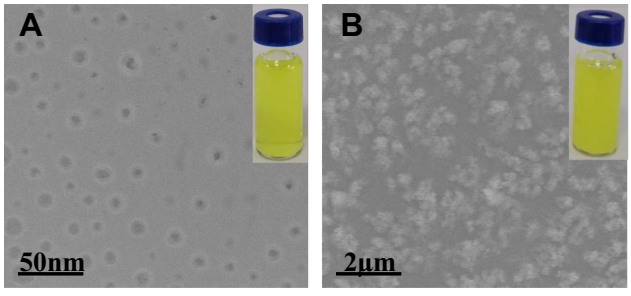

Figure 5 (**A**) TEM observation of the BTFM without adding keratin solution. (**B**) TEM observation of the interaction between BTFM and keratins (keratin solution was mixed with BTFM in equal volume and incubated in a shaker at 37 °C and 100 rpm for 1 h).

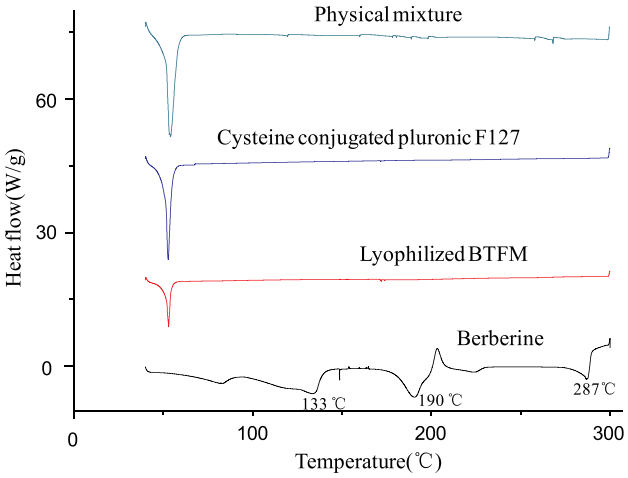

Figure 6 DSC thermograms of physical mixture of berberine and cysteine conjugated pluronic F127, cysteine conjugated pluronic F127, lyophilized BTFM as well as berberine.

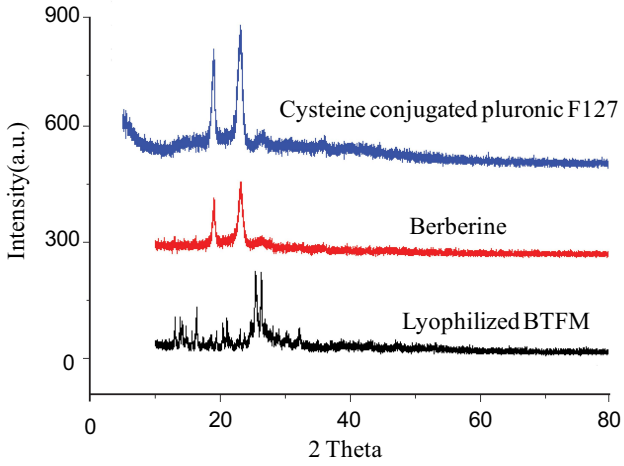

Figure 7 X-ray diffraction patterns of cysteine conjugated pluronic F127, berberine as well as lyophilized BTFM.

endothermic peak at 52°C, which corresponds to the melting point of the carrier material of the cysteine conjugated pluronic F127. The thermal behaviour of lyophilised BTFM was different from that of the physical mixtures, the characteristic endothermic peaks (at 133°C, 190°C and 287°C) of berberine disappeared completely in the lyophilised BTFM samples, while the characteristic endothermic absorption peaks of berberine were still visible in the physical mixture. The disappearance of characteristic endothermic peaks of berberine in the lyophilised BTFM samples might indicate that berberine was either encapsulated in the hydrophobic core of the micelles or completely transformed from a crystalline form to an amorphous state in the micellar core compartment.[49,50]

X-Ray Diffraction

In order to further confirm the physical existing status of the drug in the micelles, cysteine conjugated pluronic F127, pure berberine, and lyophilised BTFM were studied using XRD. Results from XRD spectra were basically consistent with those from the DSC studies (Figure 7). The crystalline nature of berberine was indicated by two sharp, narrow, diffraction peaks with the highest intensities at 19.1º and 25.3º.[51,52] Cysteine conjugated pluronic F127 exhibited two sharp peaks at 18.4º and 23.9º. Additionally, the diffraction patterns of berberine were different from those of the lyophilised BTFM. Specifically, the sharp peaks of berberine disappeared in the diffraction patterns of the lyophilised BTFM, berberine was encapsulated in the polymeric micelles in molecular or amorphous state and there was no free drug on the surface of micelles.[53] This result was consistent with the DSC results.

In the previous reports, it has also been mentioned that the crystalline molecules of berberine were converted to the amorphous state.[52,54] Likewise, as seen from the present results of characterization study of DSC and XRD, the crystalline structure of berberine was destroyed by means of micellar formulations, and transformed to the amorphous dispersions in the micellar core compartment, the results indicated that there was a good compatibility between the carriers and the drugs,[55] and the cysteine conjugated pluronic F127 is suitable for the loading of berberine. Amorphous berberine molecules have greater free energy compared to their corresponding crystalline forms. Therefore, such a physical transformation of the berberine could be contributed to enhanced solubility and dissolution rates comparing with that of crystalline berberine.[52,56] Thus, changing the crystalline nature through micellar formulations may be an ideal approach for enhancement of solubility and release of drug molecules, which may further improve skin bioavailability.

Fourier Transform Infrared Spectroscopy (FTIR)

The FTIR spectra of berberine, physical mixture of berberine and cysteine conjugated pluronic F127, berberine-loaded micelles (BTFM) and corresponding empty blank micelles are shown in Figure 8. It can be seen that pure berberine exhibits some characteristic absorption bands in the FTIR spectra. The typical characteristic absorption band at 1506.05 cm^{-1} was attributed to benzene ring of berberine.[25] The absorption bands of BTFM were similar to those of the blank micelles samples, except for the

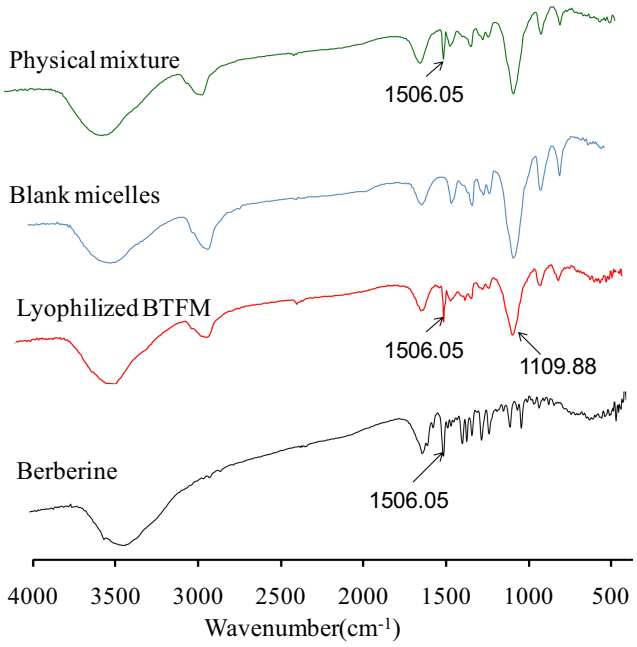

Figure 8 FTIR spectra of physical mixture of berberine and cysteine conjugated pluronic F127, blank micelles, lyophilized BTFM as well as berberine.

characteristic peaks of berberine. This results verified that berberine was successfully entrapped into the inner core of the micelles. The spectrograms of physical mixture were identical and simple overlap of berberine and cysteine conjugated pluronic F127, and the similar result was obtained in BTFM. Compared with the physical mixture, BTFM showed no new peaks or shift of the characteristic peak position, indicating that no new chemical bond was formed and some physical interactions between the berberine and polymer in the forming of BTFM.

In vitro Release of Berberine-Loaded Micelles

The release behaviour of BTFM in vitro was studied at pH 5.5 and pH 7.4 release media to simulate the release in different acidic environments of the epidermis and dermis (Figure 9A). The release of the berberine solution was almost complete at the two pH conditions for 24 h, and the release amount reached over 98%. This indicated that the dialysis bag had no retention effects on the drug. Next, in the case of formulations, there were similar burst releases of BTFM around 20% in the first 1 h at both pH 5.5 and pH 7.4. Subsequently, sustained release curves of BTFM were observed, and the cumulative release rates of berberine from BTFM at pH 5.5 and pH 7.4 for 24 h were 61.6% and 53.0%, respectively. From the release profiles, it could be found that the prepared micelles had

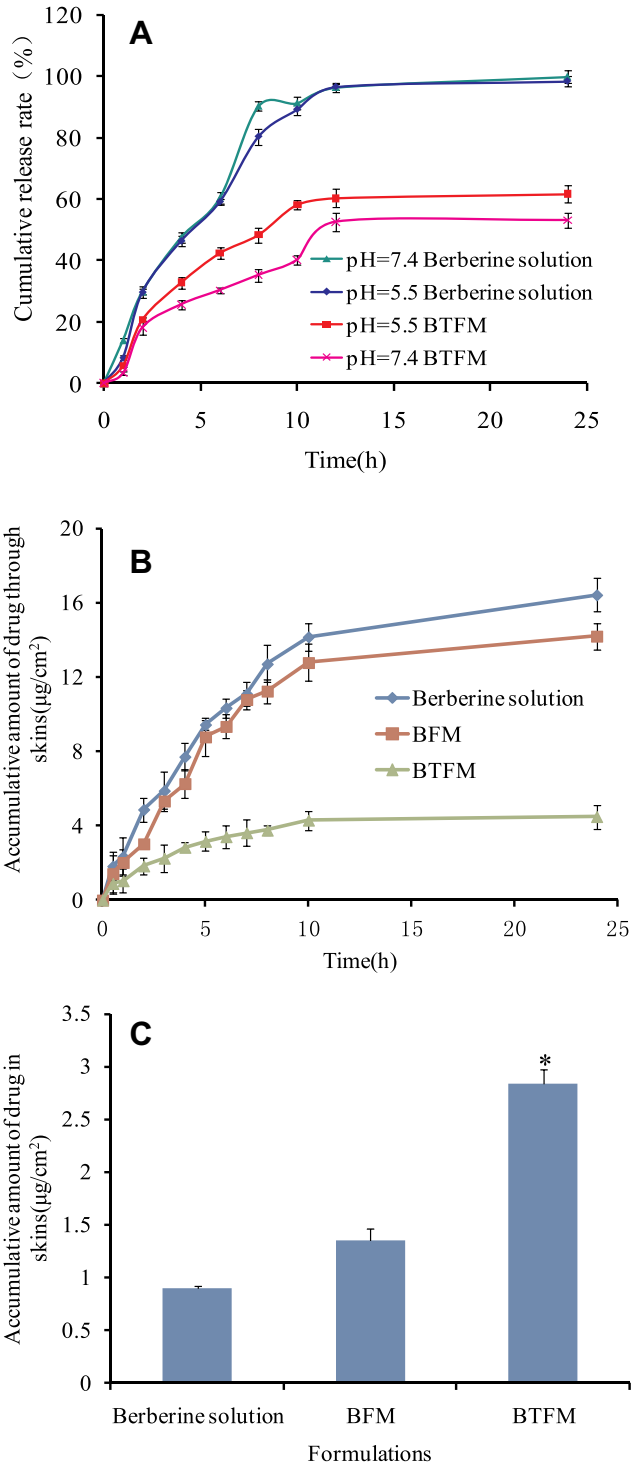

Figure 9 (**A**) In vitro profile of berberine release (mean±SD, n=3) from berberine solution and BTFM in phosphate buffer solution of pH 7.4 and pH 5.5. (**B**) In vitro permeation of berberine from BFM, BTFM and drug solution across rat skin in pH 7.4. (**C**) Berberine retention in rat skin after exposure to BFM, BTFM and drug solution for 24 h (data given as the mean ± SD, n=3; *$p < 0.05$ versus berberine solution).

both burst-release and sustained-release phases in vitro release studies. The initial burst release of berberine from the micelle particles was probably caused by drugs incorporation near the

micellar surface or drugs existing in the micro-channels of micelles.[57,58] The sustained-release behavior might be attributed to the stable incorporation of hydrophobic berberine in the core of the micelles and slow diffusion of berberine from the micelles.[59,60] Although the drug release of berberine from BTFM at pH 5.5 was faster than that at pH 7.4, there was no significant difference in release at pH 5.5 and 7.4. This finding indicates that BTFM can form a drug repository in the epidermis and dermis. Additionally, berberine released relatively rapidly from the BTFM in the acidic medium, which may be explained by the hydrophobicity of the molecule that exists in the form of hydrochloride and has certain water solubility in acidic conditions. However, berberine has poor water solubility in neutral environments and slows down its release from the formulations.[61] In addition, BTFM released more than 60% of the drug within 24 h, which suggests that the effective drug concentration was maintained in the epidermis and was beneficial to the efficacy of the drug.

As shown in Figure 9A, the BTFM had sustained release effects at pH 5.5 and 7.4. Since the pH value of the epidermis (pH 5.5) is weakly acidic,[62,63] it is necessary to determine the release mechanism of berberine from BTFM at pH 5.5. The release kinetics of BTFM were fitted by Zero-order, First-order, Higuchi and Korsmeyer-Peppas, respectively. The fitting results are shown in Table 2. The R^2 value suggested that the release kinetics of BTFM had a high degree of fit with the Higuchi and Korsmeyer-Peppas models, indicating that the drug release mechanism may be explained by Fick diffusion, which describes diffusion-based drug release from porous polymer skeleton systems.[64]

In vitro Skin Penetration and Retention Studies

Berberine has anti-inflammatory pharmacological activity and has been clinically used as a local therapeutic drug for skin diseases, including subacute dermatitis or eczema. In the treatment of local skin diseases, it is important to improve the local skin absorption of berberine and reduce its transdermal absorption. Therefore, franz diffusion cells were used to evaluate the in vitro transdermal behaviour of berberine from the BTFM that entered and passed through rat skin in order to investigate the skin retention ability of BTFM (Figure 9A). At 24 h after transdermal administration, the cumulative transdermal amount of berberine from the berberine solution, BFM and, BTFM was 16.43±0.91 μg/cm^2, 14.21±0.72 μg/cm^2, and 4.49±0.64 μg/cm^2, respectively. Additionally, the cumulative transdermal amount of BTFM was significantly decreased as compared with the cumulative transdermal amount of BFM ($p < 0.05$). This result indicated that the BTFM reduced systemic uptake, which is beneficial for the skin retention of drugs. Therefore, the BTFM may reduce the systemic side effects of drugs and improve the local treatment effect of the skin.

The purpose of the skin retention study was to determine the amount of drug that was retained in the skin area to ensure the necessary therapeutic effect. The retention of berberine preparations in the skin is shown in Figure 9B. At 24 h after administration, the skin retention of the berberine solution, BFM, and BTFM was 0.89±0.03 μg/cm^2, 1.35±0.12 μg/cm^2, and 2.83±0.14 μg/cm^2, respectively, and the skin retention of BTFM was significantly increased as compared with that of the berberine solution and BFM ($p<0.05$). Combined with the amount of cumulative retention and transdermal penetration of berberine preparations at 24 h, the ratios of the amount of cumulative retention and transdermal penetration of the berberine solution, BFM, and BTFM were 0.05, 0.09, and 0.63, respectively. This indicated that an increase in the transdermal rate of the preparation and decrease in the absolute amount of retention led to a lower proportion of retention in the total transdermal penetration amount. It appears that skin retention was maximum for BTFM when compared with the different formulations. This may be due to the fact that (1) thiolated polymers form disulphide bonds with keratin in epidermal cells, improve the skin adhesion of the preparation, and facilitate the long-term accumulation of drugs; (2) the drug was dispersed in the hydrophobic nucleus of the micelles, and its sustained drug release was conducive to reducing the transdermal absorption of the drug; or (3) polymer micelles can accumulate on the skin surface and in the hair follicles and ultimately prolong drug skin retention.[65] In conclusion, BTFM had lower transdermal absorption and significantly increased skin retention than BFM and the berberine solution, and these characteristics

Table 2 Fitting Results of Cumulative Drug Release Curve of BTFM at pH5.5 in vitro

Kinetic Model	Fitting Equation	Regression Equation	R^2
Zero order	$M_t/M_\infty=Kt$	$y=0.02325x$	0.40513
First order	$M_t/M_\infty=1-e^{-Kt}$	$y=1-e^{-0.7732x}$	0.68571
Higuchi	$M_t/M_\infty= Kt^{0.5}$	$y=0.54861\ x^{0.5}$	0.92137
Korsmeyer-Peppas	$M_t/M_\infty= Kt^n$	$y=0.20135\ x^{0.43718}$	0.94183

Notes: M_t/M_∞ is the cumulative drug release percentage at a given moment, t is the release time and K is the release constant.

are expected to reduce the risk of systemic adverse effects and are beneficial to the treatment of skin diseases.

Fluorescence Microscopy Studies

In order to study the skin retention, we prepared the thiolated pluronic F127 polymer micelles, coumarin-6 fluorescence probe-loaded thiolated pluronic F127 polymer micelles (FTFM), and pluronic F127 micelles (FFM), and the distribution of FTFM and FFM in the skin was observed using fluorescence imaging microscopy. Results from fluorescence imaging revealed that there was no fluorescence response in the skin or the preparations that did not contain coumarin-6. The fluorescence microscopic images of the longitudinal-sections of skin from the living rats used in the permeation study of FFM and FTFM are displayed in Figure 10. It can be seen from Figure 10 that after 0.5 h of administration, both the FFM group and FTFM group showed strong fluorescence in the epidermis. Specifically, the FFM group showed strong fluorescence in the deep skin and hair follicle, while the FTFM group showed no strong fluorescence in the deep skin. After administration of FFM and FTFM, respectively, for 1.0 h and 2.0 h, fluorescence was observed in both the FFM group and FTFM group in the deep skin and hair follicle areas under the epidermis; however, the fluorescence in the FTFM group was weaker in the deep skin than that in the FFM group, and the fluorescence intensity in the epidermis of the FTFM group was higher than that in the FFM group. This might be due to the formation of disulfide bond between the thiol group on the surface of FTFM and keratin of epidermal cells, which improved the retention capacity of FTFM in the epidermis, while FFM had no bioadhesive property and could enter the deep layer of skin. Therefore, although FTFM could not reach the deep layer of the skin within 0.5 h, it had a strong retention effect in the superficial layer of the skin. With the extension of the administration time, a large amount of FFM diffused through the skin and hair follicles to the deep layer of the skin, while only a small amount of FTFM was able to enter the deep skin through the skin and hair follicles. These results further confirm the skin retention effects of FTFM.

Mechanisms Underlying the Interaction Between Thiolated Pluronic F127 Micelles with Keratins

First, TEM was used to visually reveal the adsorption of BTFM on keratin molecules. As shown in Figure 5A, the TEM micrograph showed that BTFM formed spherical nanoparticles with a uniform size distribution. The particle size of the preparation as measured by TEM was 9.5±0.21 nm and the preparation was a visually clear yellow liquid. According to the TEM image, the particle size significantly increased after the addition of keratin solution to the BTFM, and the clarity of the preparation was also reduced (Figure 5B); thus, BTFM had an affinity for keratin and had interaction and adhesion with keratin.

In addition, since the reduced keratin was positively charged, the interaction between BTFM and keratin could also be studied using particle size and zeta potential measurements.[66] Figure 11 shows the changes in particle

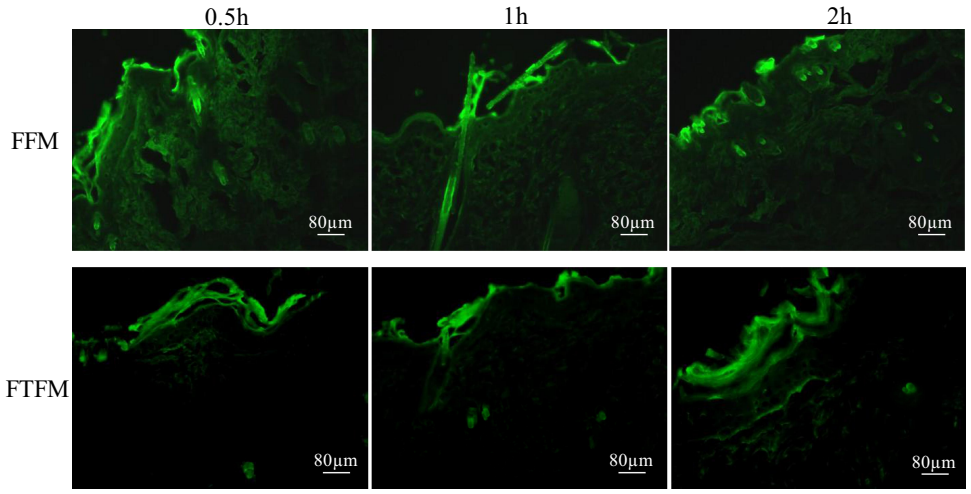

Figure 10 Fluorescence microscopic images of longitudinal-section of the living rats skin from the permeation study of FFM and FTFM.

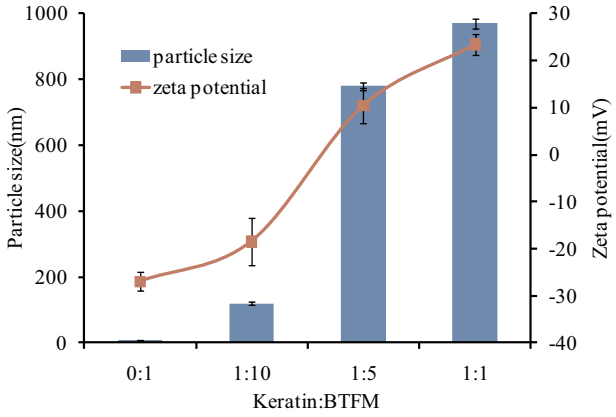

Figure 11 The zeta potential and mean particle size of the mixture of keratin and BTFM in various volume ratios at pH 7.4 (n=3).

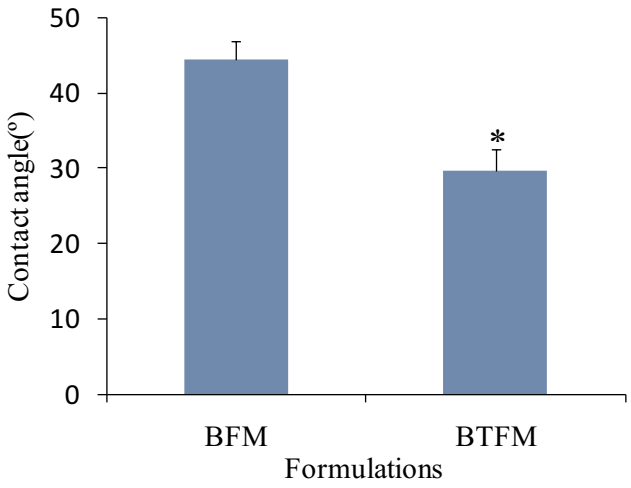

Figure 12 The contact angle of different formulation to keratins (data given as the mean ± SD, n=3; *p < 0.05 versus BFM).

size and zeta potential when BTFM and keratin were mixed at different volume proportions at pH 7.4. This figure shows that the particle size in the solution gradually increased as the ratio of keratin to BTFM increased. When the ratio of keratin to BTFM was 1:1, the particle size of BTFM increased from 9.5±0.21 nm to 970.36±8.12 nm, while the potential of BTFM changed from a negative charge (eg, −27.01±0.20 mV) to a positive charge (eg, +23.42±0.78 mV). These findings indicated that keratin had a greater affinity for BTFM, and the ionic bond effect was strong. In conclusion, the results from the size and zeta potential measurements indicate that keratin and BTFM have a certain affinity and adhesiveness.

Furthermore, the physicochemical interactions between the nanopreparations and protein molecules may include hydrogen bonds, electrostatic attractions, disulphide bonds, and hydrophobic effects, which help to consolidate and enhance the adhesion of preparations and extend the adhesion time.[67,68] Therefore, the adhesion between BTFM and keratin could be evaluated by the value of the contact angle. The results showed that the contact angle was 44.53° ±2.43° for BFM and 29.64°±3.01° for BTFM (Figure 12). Additionally, the contact angle of BTFM was lower than that of BFM, which indicated that BTFM had a high affinity for and adhered to keratin.

Acute Dermal Irritation Test

The safety of the developed formulations was evaluated through acute irritation and corrosion test. During the experiment, no erythema or edema was observed in mice with topical application of the developed formulation in the dorsocostal region (Table 3 and Figure 13). This result indicated that the formulation can be considered to be safe for topical use in humans.

Dimethyl Benzene Induced Mice Ear Edema

The results are shown in Table 4, and it was found that the BTFM significantly ($p<0.01$) suppressed the dimethyl benzene induced ear edema in mice and caused 34.47% edema inhibition. Berberine solution and BFM also significantly ($p<0.05$) inhibited the edema. Therefore, the effect of BTFM was better than that of berberine solution and BFM.

Conclusions

The berberine loaded thiolated pluronic F127 polymeric micelles were prepared via the thin film hydration method

Table 3 Appearance of Mice Belonging to the Control Group and to the Groups Treated with: Berberine Solution, BFM (Berberine-Loaded Pluronic F127 Micelles) and BTFM (Berberine-Loaded Thiolated Pluronic F127 Polymeric Micelles). Experiments Were Completed on 6 Animals for Each Group

Group	Erythema (Normal for "√")	Edema (Normal for "√")	Death/Total Animals
Control	√	√	0/6
Berberine solution	√	√	0/6
BFM	√	√	0/6
BTFM	√	√	0/6

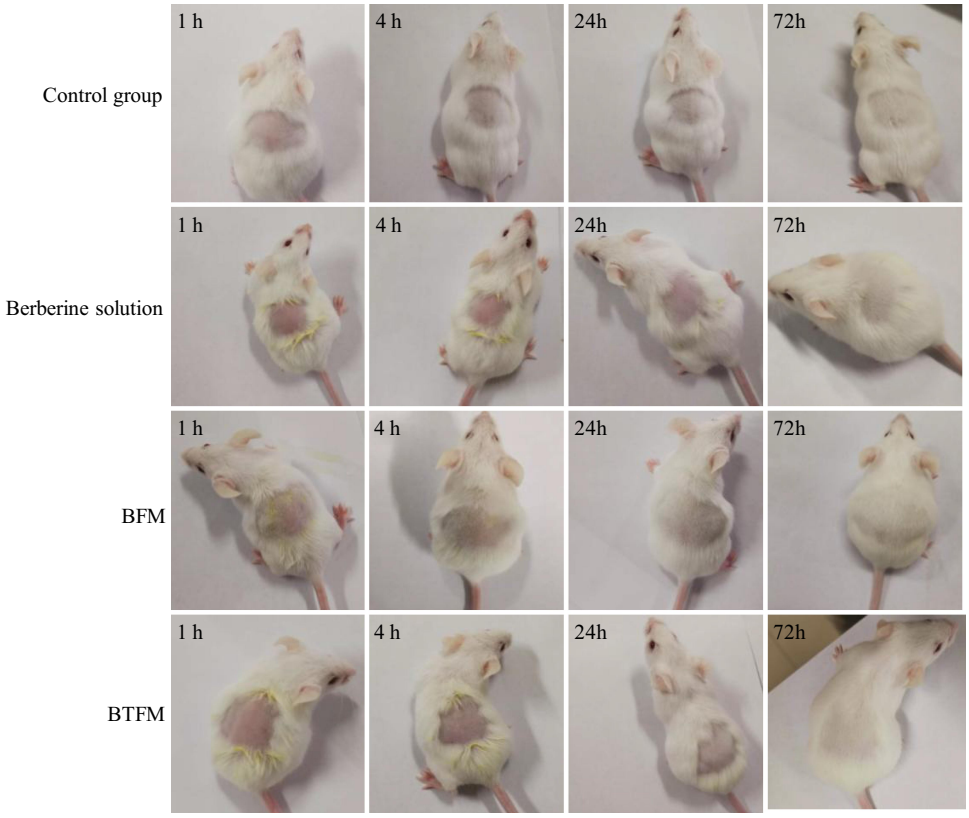

Figure 13 Acute dermal irritation/corrosion test. Mice skin appearance after 1 h, 4 h, 24 h and 72 h of observation. First line: mice treated with physiological saline (control group). Second line: mice treated with berberine solution. Third line: mice treated with BFM (berberine loaded pluronic F127 micelles). Fourth line: mice treated with BTFM (berberine loaded thiolated pluronic F127 polymeric micelles). Experiments were done on 6 animals for each group.

to improve skin permeation and retention. Overall, our results demonstrated that BTFM reduced the systemic uptake of berberine. Additionally, results from the in vitro skin penetration and retention studies showed that the cumulative transdermal amount of BTFM was decreased and the skin retention of BTFM was increased as compared with the cumulative transdermal amount and skin retention of BFM. Further, the BTFM exhibited a strong retention effect in the superficial layer of the skin. The skin retention of BTFM may contribute to the affinity of BTFM for keratin, sustained drug release, and accumulation of BTFM on the skin surface and in the hair follicles. In addition, activity tests indicated that BTFM could significantly suppress ear edema induced by dimethyl benzene, and the BTFM had a high safety profile after the acute irritation and corrosion tests. We believe that findings from this study will contribute to the development of novel polymer micelles that will improve the retention of drugs in the skin, reduce the amount of drug that enters the systemic circulation through the skin, reduce the adverse reactions caused by systemic absorption, and provide a new perspective for the treatment and prevention of skin diseases. Further evaluation is needed to illuminate its preclinical therapeutic effect.

Table 4 Effect of the Developed Formulation on Edema Induced by Dimethyl Benzene in Mice

Group	Dose (mg/kg)	Ear Edema (mg)	Inhibition Rate (%)
Control	–	41.42±10.86	–
Berberine solution	10	38.91±7.21*	6.05
BFM	10	34.77±13.31*	16.05
BTFM	10	27.14±8.54**	34.47

Notes: Data are expressed as mean ± SD of 10 mice for each group. Compared with the control group (*p<0.05, **p<0.01).

Acknowledgments

We are grateful for the financial supports from the Key Scientific Research Project of Higher Education of Henan Province (No.17B350001, No.18A230010), the National project cultivation fund of Luoyang Normal University (No.2019-PYJJ-012) and key scientific and technological project of Henan of China (202102110103).

Disclosure

The authors report no conflicts of interest for this work.

References

1. Li T, Wang P, Guo W, et al. Natural berberine-based Chinese herb medicine assembled nanostructures with modified antibacterial application. *ACS Nano*. 2019;13(6):6770–6781. doi:10.1021/acsnano.9b01346
2. Xiao CW, Ji QA, Wei Q, Liu Y, Bao GL. Antifungal activity of berberine hydrochloride and palmatine hydrochloride against microsporum canis -induced dermatitis in rabbits and underlying mechanism. *BMC Complement Altern Med*. 2015;15(1):177. doi:10.1186/s12906-015-0680-x
3. Yin J, Hou Y, Yin Y, Song X. Selenium-coated nanostructured lipid carriers used for oral delivery of berberine to accomplish a synergic hypoglycemic effect. *Int J Nanomedicine*. 2017;12:8671–8680. doi:10.2147/IJN.S144615
4. Deng J, Wu Z, Zhao Z, et al. Berberine-loaded nanostructured lipid carriers enhance the treatment of ulcerative colitis. *Int J Nanomedicine*. 2020;15:3937–3951. doi:10.2147/IJN.S247406
5. Lu KY, Lin YC, Lu HT, et al. A novel injectable in situ forming gel based on carboxymethyl hexanoyl chitosan/hyaluronic acid polymer blending for sustained release of berberine. *Carbohydr Polym*. 2019;206:664–673. doi:10.1016/j.carbpol.2018.11.050
6. Vanti G, Wang M, Bergonzi MC, Zhidong L, Bilia AR. Hydroxypropyl methylcellulose hydrogel of berberine chloride-loaded escinosomes: dermal absorption and biocompatibility. *Int J Biol Macromol*. 2020;164:232–241. doi:10.1016/j.ijbiomac.2020.07.129
7. Vanti G, Bani D, Salvatici MC, Bergonzi MC, Bilia AR. Development and percutaneous permeation study of escinosomes, escin-based nanovesicles loaded with berberine chloride. *Pharmaceutics*. 2019;11(12):12. doi:10.3390/pharmaceutics11120682
8. Arora D, Nanda S. Quality by design driven development of resveratrol loaded ethosomal hydrogel for improved dermatological benefits via enhanced skin permeation and retention. *Int J Pharm*. 2019;567:118448. doi:10.1016/j.ijpharm.2019.118448
9. Shinde UA, Parmar SJ, Easwaran S. Metronidazole-loaded nanostructured lipid carriers to improve skin deposition and retention in the treatment of rosacea. *Drug Dev Ind Pharm*. 2019;45(7):1039–1051. doi:10.1080/03639045.2019.1569026
10. Maione-Silva L, de Castro EG, Nascimento TL, et al. Ascorbic acid encapsulated into negatively charged liposomes exhibits increased skin permeation, retention and enhances collagen synthesis by fibroblasts. *Sci Rep*. 2019;9(1):522. doi:10.1038/s41598-018-36682-9
11. Kaewbanjong J, Amnuaikit T, Souto EB, Boonme P. Antidermatophytic activity and skin retention of clotrimazole microemulsion and microemulsion-based gel in comparison to conventional cream. *Skin Pharmacol Physiol*. 2018;31(6):292–297. doi:10.1159/000491756
12. Yokota J, Kyotani S. Influence of nanoparticle size on the skin penetration, skin retention and anti-inflammatory activity of non-steroidal anti-inflammatory drugs. *J Chin Med Assoc*. 2018;81(6):511–519. doi:10.1016/j.jcma.2018.01.008
13. Chin GS, Todo H, Kadhum WR, Hamid MA, Sugibayashi K. In vitro permeation and skin retention of alpha-mangostin proniosome. *Chem Pharm Bull (Tokyo)*. 2016;64(12):1666–1673. doi:10.1248/cpb.c16-00425
14. Kahraman E, Ozhan G, Ozsoy Y, Gungor S. Polymeric micellar nanocarriers of benzoyl peroxide as potential follicular targeting approach for acne treatment. *Colloids Surf B Biointerfaces*. 2016;146:692–699. doi:10.1016/j.colsurfb.2016.07.029
15. Zhang H, Zhao L, Chu L, Han X, Zhai G. Preparation, optimization, characterization and cytotoxicity in vitro of Baicalin-loaded mixed micelles. *J Colloid Interface Sci*. 2014;434:40–47. doi:10.1016/j.jcis.2014.07.045
16. Yotsumoto K, Ishii K, Kokubo M, Yasuoka S. Improvement of the skin penetration of hydrophobic drugs by polymeric micelles. *Int J Pharm*. 2018;553(1–2):132–140. doi:10.1016/j.ijpharm.2018.10.039
17. Zhou FL, Xu HM, Song ZM, Zhu L, Feng SJ, Feng RL. Alpha-linolenic acid-modified pluronic 127-CS copolymeric micelles for the skin targeted delivery of amphotericin B. *New J Chem*. 2019;43(1):444–453. doi:10.1039/C8NJ03847C
18. Yang Y, Sunoqrot S, Stowell C, et al. Effect of size, surface charge, and hydrophobicity of poly(amidoamine) dendrimers on their skin penetration. *Biomacromolecules*. 2012;13(7):2154–2162. doi:10.1021/bm300545b
19. Lapteva M, Santer V, Mondon K, et al. Targeted cutaneous delivery of ciclosporin A using micellar nanocarriers and the possible role of inter-cluster regions as molecular transport pathways. *J Control Release*. 2014;196:9–18. doi:10.1016/j.jconrel.2014.09.021
20. Bachhav YG, Mondon K, Kalia YN, Gurny R, Moller M. Novel micelle formulations to increase cutaneous bioavailability of azole antifungals. *J Control Release*. 2011;153(2):126–132. doi:10.1016/j.jconrel.2011.03.003
21. Chen CH, Lin YS, Wu SJ, Mi FL. Multifunctional nanoparticles prepared from arginine-modified chitosan and thiolated fucoidan for oral delivery of hydrophobic and hydrophilic drugs. *Carbohydr Polym*. 2018;193:163–172. doi:10.1016/j.carbpol.2018.03.080
22. Huo MR, Fu Y, Liu YH, et al. N-mercapto acetyl-N ‘-octyl-O, N “-glycol chitosan as an efficiency oral delivery system of paclitaxel. *Carbohydr Polym*. 2018;181:477–488. doi:10.1016/j.carbpol.2017.10.066
23. Zhang M, Asghar S, Jin X, et al. The enhancing effect of N-acetylcysteine modified hyaluronic acid-octadecylamine micelles on the oral absorption of paclitaxel. *Int J Biol Macromol*. 2019;138:636–647. doi:10.1016/j.ijbiomac.2019.07.114
24. Mahmood A, Lanthaler M, Laffleur F, Huck CW, Bernkop-Schnurch A. Thiolated chitosan micelles: highly mucoadhesive drug carriers. *Carbohydr Polym*. 2017;167:250–258. doi:10.1016/j.carbpol.2017.03.019
25. Wu JZ, Zhao JJ, Zhang B, et al. Polyethylene glycol-polylactic acid nanoparticles modified with cysteine-arginine-glutamic acid-lysine-alanine fibrin-homing peptide for glioblastoma therapy by enhanced retention effect. *Int J Nanomedicine*. 2014;9:5261–5271.
26. Baus RA, Leichner C, Steinbring C, Bernkop-Schnurch A. Strategies for improved hair binding: keratin fractions and the impact of cationic substructures. *Int J Biol Macromol*. 2020;160:201–211. doi:10.1016/j.ijbiomac.2020.05.131
27. Xu W, Fan X, Zhao Y, Li L. Cysteine modified and bile salt based micelles: preparation and application as an oral delivery system for paclitaxel. *Colloids Surf B Biointerfaces*. 2015;128:165–171. doi:10.1016/j.colsurfb.2015.02.031
28. Hong W, Chen D, Zhang X, et al. Reversing multidrug resistance by intracellular delivery of pluronic(R) P85 unimers. *Biomaterials*. 2013;34(37):9602–9614. doi:10.1016/j.biomaterials.2013.08.032
29. Patel V, Ray D, Bahadur A, Ma J, Aswal VK, Bahadur P. Pluronic ((R))-bile salt mixed micelles. *Colloids Surf B Biointerfaces*. 2018;166:119–126. doi:10.1016/j.colsurfb.2018.03.001
30. Basalious EB, Shamma RN. Novel self-assembled nano-tubular mixed micelles of pluronics P123, pluronic F127 and phosphatidylcholine for oral delivery of nimodipine: in vitro characterization, ex vivo transport and in vivo pharmacokinetic studies. *Int J Pharm*. 2015;493(1–2):347–356. doi:10.1016/j.ijpharm.2015.07.075
31. Jindal N, Mehta SK. Nevirapine loaded poloxamer 407/pluronic P123 mixed micelles: optimization of formulation and in vitro evaluation. *Colloids Surf B Biointerfaces*. 2015;129:100–106. doi:10.1016/j.colsurfb.2015.03.030
32. Fang XB, Zhang JM, Xie X, et al. pH-sensitive micelles based on acid-labile pluronic F68-curcumin conjugates for improved tumor intracellular drug delivery. *Int J Pharm*. 2016;502(1–2):28–37. doi:10.1016/j.ijpharm.2016.01.029

33. Zhao X, Liu P. Reduction-responsive core-shell-corona micelles based on triblock copolymers: novel synthetic strategy, characterization, and application as a tumor microenvironment-responsive drug delivery system. *ACS Appl Mater Interfaces*. 2015;7(1):166–174. doi:10.1021/am505531e
34. Sharma N, Ojha H, Pathak DP, Goel R, Sharma RK. Ex-vivo complexation, skin permeation, interaction and cytodermal toxicity studies of p-tertbutylcalix[4]arene nanoemulsion for radiation decontamination. *Life Sci*. 2017;168:65–76. doi:10.1016/j.lfs.2016.11.007
35. Patel N, Jain S, Lin S. Transdermal iontophoretic delivery of tacrine hydrochloride: correlation between in vitro permeation and in vivo performance in rats. *Int J Pharm*. 2016;513(1–2):393–403. doi:10.1016/j.ijpharm.2016.09.038
36. Liu C, Hui M, Quan P, Fang L. Drug in adhesive patch of palonosetron: effect of pressure sensitive adhesive on drug skin permeation and in vitro-in vivo correlation. *Int J Pharm*. 2016;511(2):1088–1097. doi:10.1016/j.ijpharm.2016.08.015
37. Han S, Ham TR, Haque S, Sparks JL, Saul JM. Alkylation of human hair keratin for tunable hydrogel erosion and drug delivery in tissue engineering applications. *Acta Biomater*. 2015;23:201–213. doi:10.1016/j.actbio.2015.05.013
38. Xavier-Santos JB, Felix-Silva J, Passos JGR, et al. Development of an effective and safe topical anti-inflammatory gel containing Jatropha gossypiifolia leaf extract: results from a pre-clinical trial in mice. *J Ethnopharmacol*. 2018;227:268–278. doi:10.1016/j.jep.2018.09.007
39. Peters CA, Sgrott RAG, Peters RR, et al. Production of wilbrandia ebracteata extract standardized in flavonoids and dihydrocurcubitacin and assessment of its topical anti-inflammatory activity. *Ind Crops Prod*. 2015;69:123–128. doi:10.1016/j.indcrop.2015.01.018
40. Gui X, Wang G, Zhang N, Huang B. New phenylpropanoid and other compounds from Illicium lanceolatum with inhibitory activities against LPS-induced NO production in RAW 264.7 macrophages. *Fitoterapia*. 2014;95:51–57. doi:10.1016/j.fitote.2014.02.015
41. Fan D, Zhou X, Zhao C, Chen H, Zhao Y, Gong X. Anti-inflammatory, antiviral and quantitative study of quercetin-3-O-beta-D-glucuronide in polygonum perfoliatum L. *Fitoterapia*. 2011;82(6):805–810. doi:10.1016/j.fitote.2011.04.007
42. Lapteva M, Mondon K, Moller M, Gurny R, Kalia YN. Polymeric micelle nanocarriers for the cutaneous delivery of tacrolimus: a targeted approach for the treatment of psoriasis. *Mol Pharm*. 2014;11(9):2989–3001. doi:10.1021/mp400639e
43. Alalaiwe A, Wang PW, Lu PL, Chen YP, Fang JY, Yang SC. Synergistic anti-MRSA activity of cationic nanostructured lipid carriers in combination with oxacillin for cutaneous application. *Front Microbiol*. 2018;9:1493. doi:10.3389/fmicb.2018.01493
44. Shanmugam S, Park JH, Kim KS, et al. Enhanced bioavailability and retinal accumulation of lutein from self-emulsifying phospholipid suspension (SEPS). *Int J Pharm*. 2011;412(1–2):99–105. doi:10.1016/j.ijpharm.2011.04.015
45. Kanoujia J, Kushwaha PS, Saraf SA. Evaluation of gatifloxacin pluronic micelles and development of its formulation for ocular delivery. *Drug Deliv Transl Res*. 2014;4(4):334–343. doi:10.1007/s13346-014-0194-y
46. Yang C, Zhao H, Yuan H, Yu R, Lan M. Preparation and characterization of thermosensitive and folate functionalized pluronic micelles. *J Nanosci Nanotechnol*. 2013;13(10):6553–6559. doi:10.1166/jnn.2013.7520
47. Efimova SS, Chulkov EG, Ostroumova OS. Lipid-mediated mode of action of local anesthetics on lipid pores induced by polyenes, peptides and lipopeptides. *Colloids Surf B Biointerfaces*. 2018;166:1–8. doi:10.1016/j.colsurfb.2018.02.051
48. Wang T, Wang N, Song H, et al. Preparation of an anhydrous reverse micelle delivery system to enhance oral bioavailability and anti-diabetic efficacy of berberine. *Eur J Pharm Sci*. 2011;44(1–2):127–135. doi:10.1016/j.ejps.2011.06.015
49. Zhang W, Shi Y, Chen Y, Hao J, Sha X, Fang X. The potential of pluronic polymeric micelles encapsulated with paclitaxel for the treatment of melanoma using subcutaneous and pulmonary metastatic mice models. *Biomaterials*. 2011;32(25):5934–5944. doi:10.1016/j.biomaterials.2011.04.075
50. Mohamed EA, Abu H II, Yusif RM, Suddek GM, Shaaban AAA, Badria FAE. Enhanced in vitro cytotoxicity and anti-tumor activity of vorinostat-loaded pluronic micelles with prolonged release and reduced hepatic and renal toxicities. *Eur J Pharm Sci*. 2017;96:232–242. doi:10.1016/j.ejps.2016.09.029
51. Li J, Du H, Zhang M, et al. Amorphous solid dispersion of berberine mitigates apoptosis via iPLA2beta/cardiolipin/opa1 pathway in db/db mice and in palmitate-treated MIN6 beta-cells. *Int J Biol Sci*. 2019;15(7):1533–1545. doi:10.7150/ijbs.32020
52. Shi C, Tong Q, Fang J, Wang C, Wu J, Wang W. Preparation, characterization and in vivo studies of amorphous solid dispersion of berberine with hydrogenated phosphatidylcholine. *Eur J Pharm Sci*. 2015;74:11–17. doi:10.1016/j.ejps.2015.04.001
53. Saxena V, Hussain MD. Poloxamer 407/TPGS mixed micelles for delivery of gambogic acid to breast and multidrug-resistant cancer. *Int J Nanomedicine*. 2012;7:713–721.
54. Zhaojie M, Ming Z, Shengnan W, et al. Amorphous solid dispersion of berberine with absorption enhancer demonstrates a remarkable hypoglycemic effect via improving its bioavailability. *Int J Pharm*. 2014;467(1–2):50–59. doi:10.1016/j.ijpharm.2014.03.017
55. Chadha R, Bhandari S. Drug-excipient compatibility screening–role of thermoanalytical and spectroscopic techniques. *J Pharm Biomed Anal*. 2014;87:82–97. doi:10.1016/j.jpba.2013.06.016
56. Sahibzada MUK, Sadiq A, Faidah HS, et al. Berberine nanoparticles with enhanced in vitro bioavailability: characterization and antimicrobial activity. *Drug Des Devel Ther*. 2018;12:303–312. doi:10.2147/DDDT.S156123
57. Zhang Y, Chan HF, Leong KW. Advanced materials and processing for drug delivery: the past and the future. *Adv Drug Deliv Rev*. 2013;65(1):104–120. doi:10.1016/j.addr.2012.10.003
58. Sotoudegan F, Amini M, Faizi M, Aboofazeli R. Nimodipine-loaded pluronic((R)) block copolymer micelles: preparation, characterization, in-vitro and in-vivo studies. *Iran J Pharm Res*. 2016;15(4):641–661.
59. Ding Y, Wang C, Wang Y, et al. Development and evaluation of a novel drug delivery: soluplus((R))/TPGS mixed micelles loaded with piperine in vitro and in vivo. *Drug Dev Ind Pharm*. 2018;44(9):1409–1416. doi:10.1080/03639045.2018.1472277
60. Hu X, Han R, Quan LH, Liu CY, Liao YH. Stabilization and sustained release of zeylenone, a soft cytotoxic drug, within polymeric micelles for local antitumor drug delivery. *Int J Pharm*. 2013;450(1–2):331–337. doi:10.1016/j.ijpharm.2013.04.007
61. Ji HF, Shen L. Molecular basis of inhibitory activities of berberine against pathogenic enzymes in alzheimer's disease. *ScientificWorldJournal*. 2012;2012:823201. doi:10.1100/2012/823201
62. Voegeli R, Gierschendorf J, Summers B, Rawlings AV. Facial skin mapping: from single point bio-instrumental evaluation to continuous visualization of skin hydration, barrier function, skin surface pH, and sebum in different ethnic skin types. *Int J Cosmet Sci*. 2019;41(5):411–424. doi:10.1111/ics.12562
63. Jansen van Rensburg S, Franken A, Du Plessis JL. Measurement of transepidermal water loss, stratum corneum hydration and skin surface pH in occupational settings: a review. *Skin Res Technol*. 2019;25(5):595–605. doi:10.1111/srt.12711
64. Fernandez-Colino A, Bermudez JM, Arias FJ, Quinteros D, Gonzo E. Development of a mechanism and an accurate and simple mathematical model for the description of drug release: application to a relevant example of acetazolamide-controlled release from a bio-inspired elastin-based hydrogel. *Mater Sci Eng C Mater Biol Appl*. 2016;61:286–292. doi:10.1016/j.msec.2015.12.050

65. Desai P, Patlolla RR, Singh M. Interaction of nanoparticles and cell-penetrating peptides with skin for transdermal drug delivery. *Mol Membr Biol*. 2010;27(7):247–259. doi:10.3109/09687688.2010.522203
66. Cheng Z, Chen X, Zhai D, et al. Development of keratin nanoparticles for controlled gastric mucoadhesion and drug release. *J Nanobiotechnology*. 2018;16(1):24. doi:10.1186/s12951-018-0353-2
67. Khutoryanskiy VV. Advances in mucoadhesion and mucoadhesive polymers. *Macromol Biosci*. 2011;11(6):748–764. doi:10.1002/mabi.201000388
68. Osmani N, Labouesse M. Remodeling of keratin-coupled cell adhesion complexes. *Curr Opin Cell Biol*. 2015;32:30–38. doi:10.1016/j.ceb.2014.10.004